

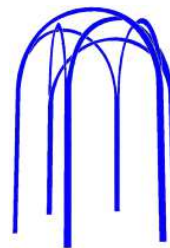


Report series ISSN 0284 – 2769 of

THE SVEDBERG LABORATORY and
DEPARTMENT OF RADIATION SCIENCES
UPPSALA UNIVERSITY

Box 533, S-751 21 Uppsala, Sweden

<http://www.tsl.uu.se/>



TSL/ISV-95-0214

August 1999

Non-perturbative Parton Distributions in the Proton¹

A. Edin^a, G. Ingelman^{ab}, K. Torokoff^b

^a Deutsches Elektronen-Synchrotron DESY, Hamburg, Germany

^b High Energy Physics, Uppsala University, Sweden, www3.tsl.uu.se/thep

Abstract: A model for the parton distributions in hadrons is derived from simple physical arguments leading to an analytical expression for the valence distributions. The sea parton distributions arise mainly from pions in hadronic fluctuations. Evolving from a low Q_0^2 scale with DGLAP gives the proton structure function $F_2(x, Q^2)$ in good agreement with DIS data. An extension of the model to describe intrinsic charm quarks in the proton is discussed.

¹In proceedings ‘Monte Carlo generators for HERA physics’, DESY-PROC-1999-02, www.desy.de/~heramc

Non-perturbative Parton Distributions in the Proton²

A. Edin^a, G. Ingelman^{ab}, K. Torokoff^b

^a Deutsches Elektronen-Synchrotron DESY, Hamburg, Germany

^b High Energy Physics, Uppsala University, Sweden, www3.tsl.uu.se/thep

Abstract: A model for the parton distributions in hadrons is derived from simple physical arguments leading to an analytical expression for the valence distributions. The sea parton distributions arise mainly from pions in hadronic fluctuations. Evolving from a low Q_0^2 scale with DGLAP gives the proton structure function $F_2(x, Q^2)$ in good agreement with DIS data. An extension of the model to describe intrinsic charm quarks in the proton is discussed.

1 Introduction

When calculating cross sections for hard processes with incoming hadrons, the structure of the hadrons is described by parton distributions. The dependence of the parton distributions on the hard scale Q of the interaction is described by perturbative QCD evolution. However, their dependence on the momentum fraction x at the lower limit for applying perturbative QCD, $Q_0 \approx 0.5 - 2$ GeV, cannot be calculated perturbatively and must therefore be obtained by other means.

The easiest solution is to fit a parameterization [1, 2, 3], *e.g.* of the form $f_i(x, Q_0) = N_i x^{a_i} (1-x)^{b_i} (1+c_i\sqrt{x}+d_i x)$, to experimental data and then use these functions when calculating cross sections. The problem with this approach is that the parameters in these functions have no direct physical meaning, making it difficult to interpret the results.

To gain understanding of non-perturbative QCD and the structure of hadrons we have developed a physical model [4, 5] for the parton distributions at Q_0 . The model is here briefly described together with our latest developments.

2 The model

The basic assumption in the model is that the probe resolving the hadron has much higher resolution than the size of the hadron. The probe will then see *free quarks and gluons* in quantum fluctuations of the hadron. As illustrated in Fig. 1a, the measuring time is short compared to the life-time of the fluctuation which is given by the confinement scale. This makes it possible to describe the formation of the fluctuation independently of the measuring process.

²In proceedings ‘Monte Carlo generators for HERA physics’, DESY-PROC-1999-02, www.desy.de/~heramc

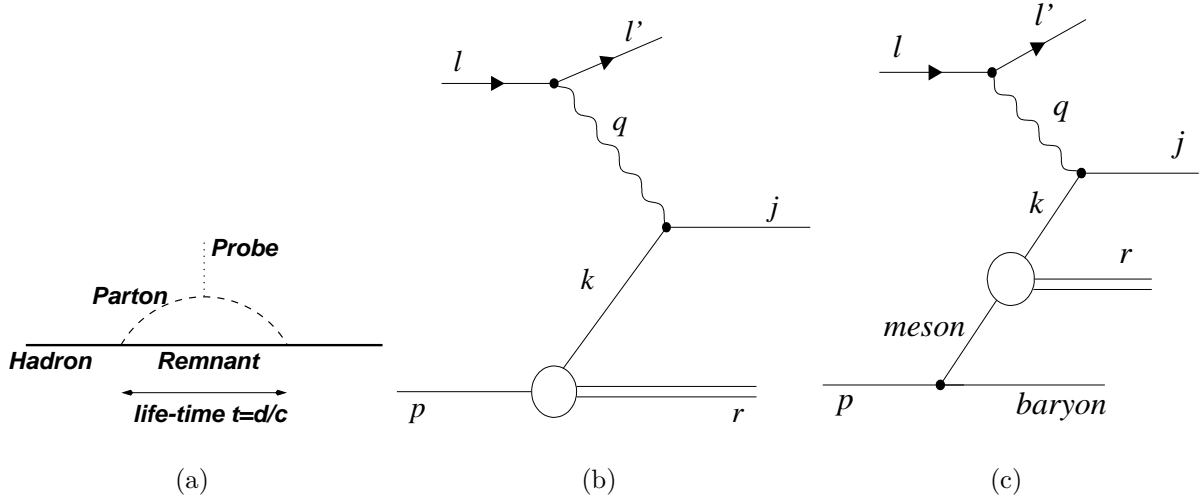


Figure 1: (a) Time scales in probing a parton in a hadron. Kinematics and four-vectors for scattering on (a) a valence parton and (b) a sea parton in a hadronic fluctuation.

Our approach only intends to provide the probability distribution of the four-momentum k of a single probed parton. All other information in the hadron wave function is neglected, treating the other partons collectively as a remnant with four-momentum r , see Fig. 1b. The parton distribution is described using the light-cone momentum fraction $x = \frac{k_+}{p_+}$ which the parton has in the initial hadron. Since x is invariant under boosts in the z direction, the same will be true for the calculated parton distributions.

It is most convenient to describe the fluctuations in the hadron rest frame where there is no preferred direction and hence spherical symmetry. The momentum distribution of the partons should therefore be spherically symmetric. The shape of the momentum distribution should be close to a Gaussian as a result of the many interactions binding the parton in the hadron. The typical width of this distribution should be a few hundred MeV from the Heisenberg uncertainty relation applied to the hadron size. The Gaussian momentum distribution also has phenomenological support. The Fermi motion in the proton provides the ‘primordial transverse momentum’, which has been extracted from DIS data and found to be well described by a Gaussian distribution of a few hundred MeV width [6].

2.1 Valence partons

The probability distribution in momentum space for finding one parton i with mass m_i is therefore given by the Gaussian

$$f_i(k) = N(\sigma_i, m_i) e^{-\frac{(k_0 - m_i)^2 + k_1^2 + k_2^2 + k_3^2}{2\sigma_i^2}}, \quad (1)$$

where $\sigma = \frac{1}{d_h} \approx m_\pi$ is the inverse of the confinement length scale, *i.e.* the hadron diameter. The Gaussian in the energy component comes from the limited time the parton can be ‘free’.

The parton distributions must fulfill a number of constraints. The normalization for valence quarks is given by the sum rules and for the gluons by the momentum sum rule, *i.e.*

$$\int_0^1 f_i(x) dx = n_i \quad \text{and} \quad \sum_i \int_0^1 x f_i(x) dx = 1. \quad (2)$$

There are also the kinematic constraints $m_i^2 \leq j^2 < W^2$ and $r^2 > \sum_i m_i^2$ given by the final parton j being on-shell or time-like and the remnant having to include the remaining partons. This also leads to $0 < x < 1$.

The parton model requires that W is well above the resonance region and that the resolution of the probe is much larger than the size of the hadron, *i.e.* $W \gg m_p$ and $Q_0 \gg \sigma_i$. The scale of the probe must also be large enough, $Q_0 \gg \Lambda_{QCD}$, for perturbative QCD to describe the evolution of the parton distributions from the starting scale Q_0 .

In [4] we integrated eq. 1 numerically to find the parton distributions since the kinematic constraints are quite complicated in general. The problem is much simpler if the transverse momenta and the masses of the partons are neglected. It is then possible to derive [7] an analytical expression for the parton distributions,

$$f_i(x) = N'(\tilde{\sigma}_i) \exp\left(-\frac{x^2}{4\tilde{\sigma}_i^2}\right) \operatorname{erf}\left(\frac{1-x}{2\tilde{\sigma}_i}\right) \quad \text{where} \quad \tilde{\sigma}_i = \frac{\sigma_i}{m_h} = \frac{1}{d_h m_h} \approx \frac{m_\pi}{m_h}. \quad (3)$$

The valence parton distributions for hadrons are here determined simply by the mass and size of the hadron!

The resulting valence distributions for the proton ($\tilde{\sigma} \approx 0.15$) and the pion ($\tilde{\sigma} \approx 1$) are very reasonable as shown in Fig. 2. Note that the pion distributions are very similar to $xf(x) = 2x(1-x)$ and that one third of the pion momentum is carried by gluons.

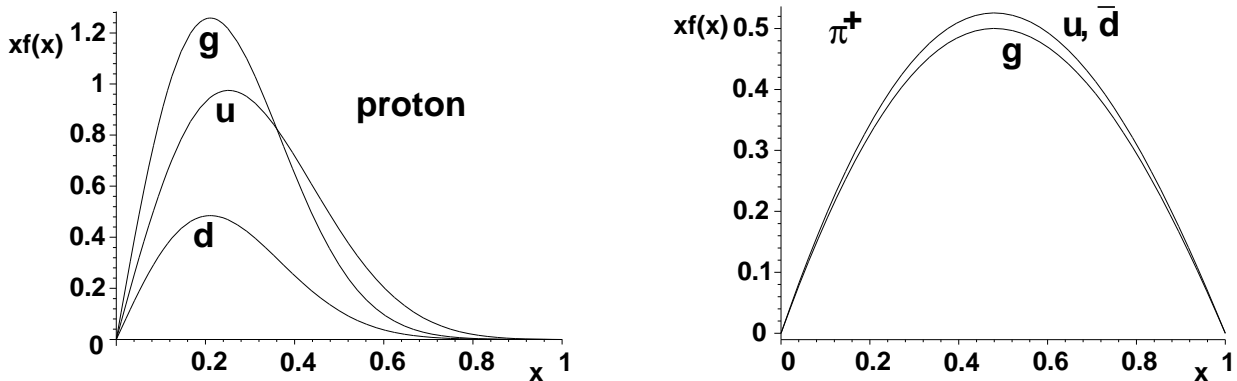


Figure 2: Valence distributions at $Q_0 \approx 0.85$ GeV in the proton and π^+ .

2.2 Sea partons

The sea partons are described by hadronic fluctuations as illustrated in Fig. 1c. For example, the proton fluctuates into $|p\pi^0\rangle + |n\pi^+\rangle + \dots$ and the scattering is on a valence parton in one of the two hadrons, most importantly the pion. The sea quark momentum distribution is obtained as the convolution of the valence parton in the pion, which was already obtained from the model, with the momentum distribution of the pion in the hadronic fluctuation. The latter is assumed to follow from the same model, *i.e.* using a spherically symmetric Gaussian momentum distribution in the proton rest frame. However, the width $\sigma_\pi \approx 50$ MeV is smaller, related to the longer range of pionic strong interactions or the size of the virtual pion cloud around a proton.

3 Proton structure function and DIS data

Using these valence and sea parton x distributions at Q_0 , next-to-leading order DGLAP evolution in the CTEQ computer program [1] was applied to obtain the parton distributions at larger Q . The proton structure function $F_2(x, Q^2)$ was then calculated and compared with deep inelastic scattering data as illustrated in Fig. 3. The model curves were obtained [4] using the full numerical integration including effects from masses, transverse momenta and exact kinematic constraints rather than with the simplified analytical expression in eq. (3). Furthermore, the model parameters are here fitted to the data giving $Q_0 = 0.85$ GeV, $\sigma_u = 180$ MeV, $\sigma_d = 150$ MeV, $\sigma_g = 135$ MeV, $\sigma_\pi = 52$ MeV and 7.7% of the proton momentum carried by sea partons (*i.e.* pion fluctuation normalization). These values are in very good agreement with the definite expectations of the model. In particular, the values σ_i in eq. (1) corresponds to the Fermi motion in the proton. (Since σ applies in each dimension, one obtains a two-dimensional distribution with $\langle k_\perp^2 \rangle = 2\sigma^2$ in agreement with data on the primordial transverse momentum.) One may note that the u -quark distribution has a $\sim 20\%$ larger width, which may correspond to a correspondingly smaller available region due to the Pauli exclusion principle.

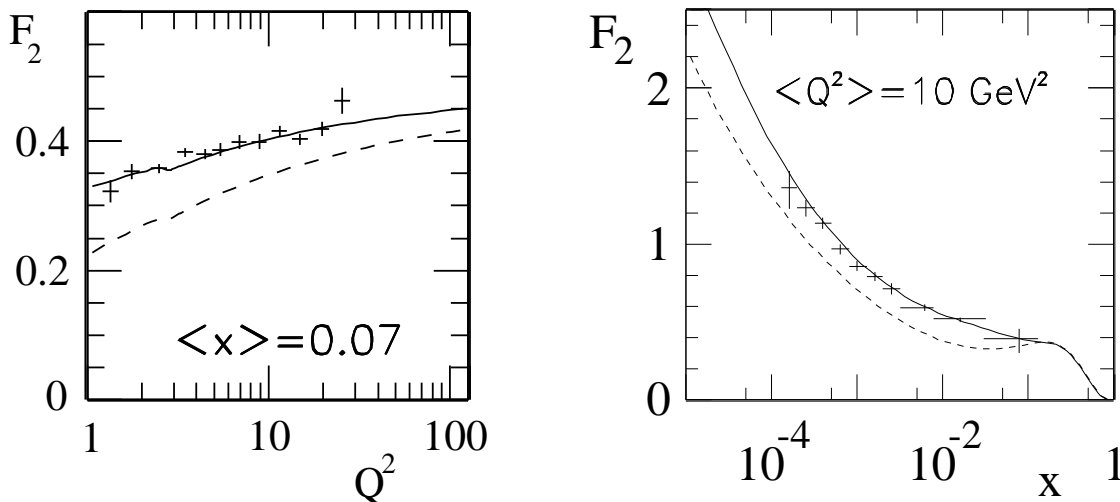


Figure 3: Data from NMC [10] (left) and ZEUS [9] (right) on the proton structure function $F_2(x, Q^2)$ compared to the model with valence partons only (dashed) and including sea partons (full). Extracted from [4] where larger x, Q^2 regions are examined.

The model does remarkably well in view of its simplicity and few parameters (6). Of course, conventional parton density parameterizations give better fits, probably mainly due to their many more parameters (≈ 20). The main advantage with our approach is that it provides a model that not only gives a good representation of data, but also provides new insights through a physical model for the non-perturbative input distributions.

The main part of the proton structure is determined by the valence distributions, but the sea gives an important contribution at small x . For $Q^2 < 1 \text{ GeV}^2$ the DIS formalism and the partonic interpretation of F_2 are not straightforwardly applicable. Photoproduction and resolved photon processes must here be included in the theoretical description of the data. More generally, parton distributions can only be used when the hadron is resolved by a sufficiently large scale. Hence, for $Q^2 < Q_0^2$ our parton distribution model can only be applied for processes with some other hard scale, *e.g.* jets in photoproduction, and not to obtain the total photon-proton cross section or F_2 extracted from it.

4 Intrinsic charm

Following the model described above we have made a detailed investigation [12] on how it can be extended to describe intrinsic charm quarks in the proton. The main results and their comparison with the original intrinsic charm model of Brodsky et al. [13] are briefly discussed here. Studies on the possibility to observe intrinsic charm in DIS have been presented earlier [14].

The idea that our model for parton distributions may be applied to describe intrinsic charm is obvious, but there are problems of both conceptual and technical nature. Extending the model for generating sea quarks through hadronic fluctuations, illustrated in Fig. 1c, means that one should consider fluctuations $|p\rangle \rightarrow |\Lambda_c^+ \bar{D}^0\rangle + \dots$. In old-fashioned perturbation theory the particles are on-shell and the fluctuation is suppressed by a factor proportional to $1/\Delta E^2$. This provides a description with energy fluctuation in the hadron basis (EFH).

The large mass of the charm quark and charm hadrons means a large fluctuation ΔE and one could argue that the fluctuation is correspondingly short-lived and that the hadron basis is not suitable since hadron states are not formed. One should then picture the charm quark as coming directly from the proton, as in Fig. 1b, with a remnant containing the charm anti-quark (or vice versa) to conserve the charm quantum number. This gives a description with energy fluctuation in the parton basis (EFP).

An alternative description is to impose energy-momentum conservation, which means that in the hadron (parton) basis the charm meson (quark) is off-shell. The charm baryon (remnant) is external to the hard scattering process and should therefore be on-shell. (The remnant can be slightly off-shell if one allows it to pick up some energy in the hadronisation process.) This provides two model alternatives with energy conservation in the hadron or parton basis (ECH and ECP).

The kinematic constraints are imposed as previously, but they become harder due to the large charm mass. In fact, the ECH model is then not kinematically allowed. The results of the other model variations are shown in Fig. 4, with and without the kinematic constraints applied. In case of fluctuations in a parton basis there is quark-anti-quark symmetry, $xc(x) = x\bar{c}(x)$, while for hadronic fluctuations this is not the case since the \bar{D} meson is softer than the Λ_c baryon due to its lower mass.

As shown in Fig. 4a, the different model variations result in somewhat different charm distributions. However, if the kinematic constraints are not applied, then they give essentially the same x -distributions as demonstrated in Fig. 4b. They are also then quite similar to the x -distribution in the original intrinsic charm model [13] where these kinematic constraints are not accounted for. The sensitivity of our results on the treatment of the charm quark mass and the constraints demonstrate the importance of taking them properly into account to ensure a kinematically allowed final state.

The results of the models have been studied in more detail [12] by examining the four-vectors in the process. As expected, the incoming quark k^2 is almost on-shell in the energy fluctuation schemes, while in the energy conserving scheme it is off-shell and negative. In ECP, the j^2 distribution peaks at m_c^2 and falls very quickly for larger values. In EFP and EFH, however, j^2 is larger. This may only be an artifact which can be avoided in the model, but it can also signal that perturbative gluon emission must be taken into account. If so, also boson-gluon fusion should be included for consistency and then perturbative charm production would enter

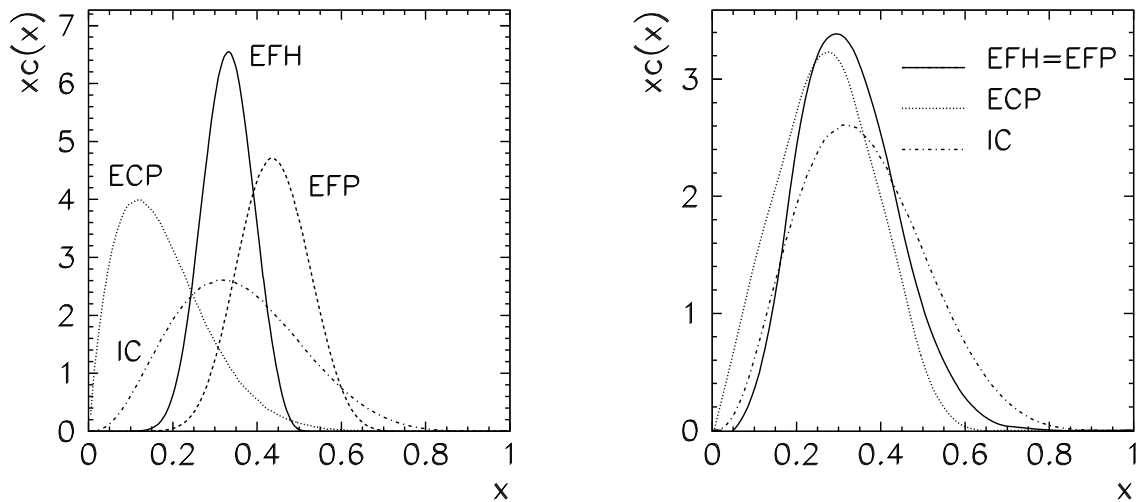


Figure 4: Momentum-weighted distributions $xc(x)$ for intrinsic charm in the proton obtained from variations of our model (EFH and EFP with energy fluctuation in hadron and parton basis, respectively, and ECP with energy conservation in parton basis) with (left) and without (right) taking into account kinematic constraints. Comparison with the original intrinsic charm (IC) model of Brodsky et al. (without constraints). All curves are normalized to unity area.

such that one would have to define a suitable factorization to disentangle the non-perturbative intrinsic charm component.

Our results here and in [12] are therefore only a first step towards a realistic model for intrinsic charm based on our general idea for deriving parton distributions.

5 Conclusions and outlook

We have shown that our new model for parton momentum distributions in hadrons is reasonable and can reproduce the measured proton structure function. They can therefore be used as an alternative to the conventional parameterizations in practical calculations of hard processes and in Monte Carlo generators. The advantage of the physical model over the parameterizations is that it provides insights on the non-perturbative dynamics embodied in the model.

The experimentally observed [11] flavour asymmetric sea with $\bar{d} > \bar{u}$ may be accounted for by including all pion fluctuations, but the numerical details remain to be investigated. The hadronic fluctuations may also be used to develop a model for the dynamics of leading baryon production (*cf.* Fig. 1c).

The application of the model to other hadrons than the proton will be presented elsewhere [7], but the results cannot be as directly and precisely tested as in deep inelastic scattering on the nucleon. However, data on the pion structure are available from Drell-Yan processes in pion beam experiments.

Applying the model to charm in the proton is interesting, but more complicated due to the large charm mass. Although reasonable results are obtained, the x -distribution depends on the details in the treatment of the charm quark mass effects and the related kinematic constraints imposed to ensure an allowed final state. The proton remnant system plays an important role in this respect such that its dynamics may be essential for developing a realistic model.

References

- [1] H.L. Lai et al., *Phys. Rev. D* **55**, 1280 (1997);
H.L. Lai et al., hep-ph/9903282
- [2] M. Glück et al., *Eur. Phys. J. C* **5**, 461 (1998)
- [3] A.D. Martin et al., *Eur. Phys. J. C* **4**, 463 (1998)
- [4] A. Edin, G. Ingelman, *Phys. Lett. B* **432**, 402 (1998)
- [5] A. Edin, G. Ingelman, proceedings of DIS99 to appear in Nucl. Phys. B (Proc.Suppl.)
- [6] G. Ingelman et al., *Nucl. Phys. B* **206**, 239 (1982)
J.J. Aubert et al., EMC collaboration, *Phys. Lett. B* **119**, 233 (1982)
M. Arneodo et al., EMC collaboration, *Phys. Lett. B* **149**, 415 (1984)
- [7] A. Edin, in preparation
- [8] M. Arneodo et al., *Phys. Lett. B* **364**, 107 (1995)
- [9] M. Derrick et al., ZEUS collaboration, *Z. Phys. C* **72**, 399 (1996)
- [10] M. Arneodo et al., NMC coll., *Phys. Lett. B* **364**, 107 (1995)
- [11] J.C. Peng et al., FNAL E866 collaboration, *Phys. Rev. D* **58**, 92004 (1998)
- [12] K. Torokoff, ‘Charm and strange quark contributions to the proton structure’, Master thesis, Uppsala University, TSL/ISV-99-0204
- [13] S.J. Brodsky, et al., *Phys. Lett. B* **93**, 451 (1980)
S.J. Brodsky, C. Peterson, *Phys. Rev. D* **23**, 2745 (1981)
- [14] G. Ingelman, L. Jönsson, M. Nyberg, *Phys. Rev. D* **47**, 4872 (1993)
G. Ingelman, M. Thunman, *Z. Phys. C* **73**, 505 (1997)